UMYU Scientifica, Vol. 2 NO. 4, December 2023, Pp 179 – 188
https://doi.org/10.56919/usci.2324.022
ISSN: 2955 – 1145 (print); 2955 – 1153 (online)
A periodical of the Faculty of Natural and Applied Sciences, UMYU, Katsina

ORIGINAL RESEARCH ARTICLE

Adsorption and inhibitive effect of N-[(4{[(Z)-(4-hydroxy phenyl) methylidene] amino} phenyl) sulfonyl acetamide on the corrosion of mild steel in HCl medium

Chikezie Ogueji[1], Okoche K. Amadi[2] Divine C. Oranuka[1] and Chineye A. Onwuka[1].
[1]Department of Chemistry, Alex Ekwueme Federal University, Ndufu-Alike, P. M. B. 1010 Abakiliki, Ebonyi State, Nigeria.
[2]Department of Chemistry, Michael Okpara University of Agriculture Umudike, Abia State, Nigeria.

ARTICLE HISTORY
Received Octorber 02, 2023.
Accepted November 30, 2023.
Published December 30, 2023.

KEYWORDS
Inhibition; adsorption isotherm; SEM; thermodynamics

ABSTRACT
In this study, the inhibitive effects of Schiff's base, N-[(4{[(Z)-(4-hydroxy phenyl) methylidene] amino} phenyl) sulfonyl acetamide (4-HPMAPSA) on mild steel corrosion in 1.0 M $HCl_{(aq)}$ at different temperatures were investigated using weight loss and scanning electron microscope. The Fourier transform infrared spectrum and X-ray diffraction pattern of 4-HPMAPSA were obtained. It was found that the inhibition effectiveness of 4-HPMAPSA relies on the temperature, 4-HPMAPSA concentration and exposure period. 4-HPMAPSA hinders mild steel corrosion and exhibits a maximum inhibitive efficiency of 88.5 % at 0.5 g of 4-HPMAPSA at 303 K. The activation energy (Ea) value (45.0 to 52.3 $kJmol^{-1}$) with an average of 47.7 $kJmol^{-1}$ was obtained for the 4-HPMAPSA-inhibited reaction and 35.1 $kJmol^{-1}$ for the uninhibited. The thermodynamic values calculated for the 4-HPMAPSA-inhibited reaction show that the process is spontaneous and endothermic. With an R^2 value of 0.9646 to 0.9999, Langmuir isotherm best described the 4-HPMAPSA uptake behaviour.

INTRODUCTION

The gradual deterioration or destruction of metals by chemical or electrochemical reactions with their environment is called corrosion (Guruprasad et al., 2020). It is a natural process that converts a refined metal into a more chemically stable oxide. It is an afflicting problem associated with every use of metals. Mild steel has many applications in industrial installations and equipment owing to its mechanical properties; however, this metal corrodes easily when it comes in contact with an acidic solution (Ikeuba et al., 2015), leading to significant economic losses (Asmara and Kurniawan, 2018, Betti et al. 2023). Several measures have been taken to control the menace of metal deterioration, and one of the important methods or processeses is corrosion inhibitors (Onwu et al., 2016). Corrosion inhibitors are compounds which control, reduce or prevent reactions between metals and corrosive media (Chahul et al., 2018).

Most effective corrosion inhibitors are expensive, toxic and have adverse effect on the environment. The use of these inhibitors for corrosion inhibition has been restricted due to these properties (Pathak and Pratiksha, 2016). The toxicity and incompatibility of most corrosion inhibitors with human health and environment are sufficient inadequacies that have provoked a genuine and concerted search for their replacement (Ofuyekpone et al., 2021). Most well-known and effective organic inhibitors that have been produced and used for the corrosion inhibition of metals are compounds with N, O, S, and P atoms and aromatic rings or compounds (Kavitha and Gunavathy, 2014). In addition to having good corrosion inhibition properties, organic inhibitors are reliable, safer, biocompatible and eco-friendly when compared with their inorganic counterparts (Onwu et al., 2016).

Interestingly, Schiff's bases could be considered one of the most important types of organic inhibitors and have proven to offer the replacement needed to replace their toxic counterparts. The most effective acidic corrosion inhibitors for many metals and alloys are organic compounds containing electronegative atoms (nitrogen, oxygen, Sulphur, phosphorus, etc.) and unsaturated bonds (such as double). Kumari et al. (2014) reported that Schiff base –(RC=NR-) has both features (lone pair of electrons on nitrogen and double bond) combined with their structure, showing extraordinary inhibition characteristics for mild steel in an acid medium. They play significant roles by blocking the active sites when adsorbed on the surface, thereby lowering the effect of the corrodent (Hegazy et al., 2014; Abdallaha et al., 2016). The inhibitory potential of a number of Schiff bases in acidic solutions have been discovered such as 4-hydroxyl phenyl

Correspondence: Chikezie Ogueji. Department of Chemistry, Alex Ekwueme Federal University, Ndufu-Alike, P. M. B. 1010 Abakiliki, Ebonyi State, Nigeria. ✉ ogueji.chikezie@funai.edu.ng
How to cite: Ogueji, C., Amadi, O. K., Oranuka, D. C., & Onwuka, C. A. (2023). Adsorption and inhibitive effect of N-[(4{[(Z)-(4-hydroxy phenyl) methylidene] amino} phenyl) sulfonyl acetamide on the corrosion of mild steel in HCl medium. *UMYU Scientifica*, 2(4), 179 – 188. https://doi.org/10.56919/usci.2324.022

methylidene-2-(1-phenyl ethylidene) hydrazine carbothioamide and 4-hydroxy phenyl [methylidene] amino-3, 4- dimethyl-5-phenyl cyclo pent-2-en-1-one (Onwu et al., 2016; Ekuma et al., 2017); N,N'-bis-(1-hydroxyphenylimine)-2,5-thiophenedicarboxaldehyde (Wanees and Seda, 2019); 3-((5-mercapto-1,3,4-thiadiazol-2-yl) imino)indolin-2-one (Betti et al., 2023) and 2-amino-9-(1H-indol-3-yl)-4-(4-methoxyphenyl)-7-oxo1,7-dihydropyrido[1,2-b][1,2,4]triazepine-3,8,10-tricarbonitrile and ethyl 2-amino-8,10-dicyano-9-(2-hydroxy3- methoxyphenyl)-4-(4-methoxyphenyl)-7-oxo-1,7-dihydropyrido[1,2-b][1,2,4]triazepine-3-carboxy late (Paul at et al., 2021).

The Schiff's base, N-[(4{[(Z)-(4-hydroxy phenyl) methylidene]amino}phenyl) sulfonyl] acetamide (4-HPMAPSA) has not been investigated or reported for corrosion inhibition of mild steel in any medium. For the present research, FT-IR spectroscopy, SEM studies, X-ray diffraction and weight loss studies of corrosion of mild steel in the absence and presence of different concentrations of 4-HPMAPSA in 1 M HCl solution were carried out. The structure of N-[(4{[(Z)-(4-hydroxy phenyl) methylidene]amino}phenyl) sulfonyl] acetamide (4-HPMAPSA) is presented in Scheme 1.

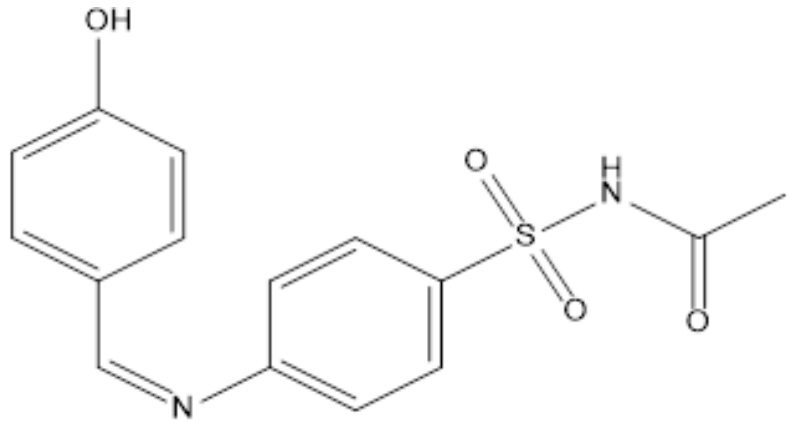

N-[(4{[(Z)-(4-hydroxy phenyl) methylidene] amino}phenyl) sulfonyl] acetamide

Scheme 1: 4-HPMAPSA

MATERIALS AND METHODS

Materials

The Schiff's base, N-[(4{[(Z)-(4-hydroxy phenyl) methylidene] amino} phenyl) sulfonyl]acetamide was synthesised through a condensation reaction. This was carried out through condensation reaction by refluxing 4-hydroxybenzaldehyde (1.22 g, 0.01 mol) with sulphacetamide (2.14 g, 0.01 mol) in the presence of ethanol. Thin-layer chromatography was used to monitor the reaction. The product was washed with a 5-10% ethylacetate-hexane mixture.

The mild steel employed for this work was of composition (wt %) P (0.36), C (0.15), Mn (0.6), Si (0.031) and Fe (98.85). The sheet material was press-cut into coupons of size 3 cm x 2 cm x 0.1 cm for each sheet. Each coupon was washed with ethanol, dried in acetone and stored in moisture-free desiccators until the time of use. A 1.0 M $HCl_{(aq)}$ was used for the gravimetric studies.

Characterisation

The N-[(4{[(Z)-(4-hydroxy phenyl) methylidene] amino} phenyl) sulfonyl]acetamide was analysed using FTIR spectrum obtained from Frontier Perkin Elmer spectrophotometer in the range of 400 to 4000 cm^{-1}. X-ray diffraction pattern of (4-HPMAPSA) was obtained using an X-ray diffractometer (model: Bruker Smart 1000 CCD diffractometer). Scanning electron micrographs were obtained for the corroded coupons using a scanning electron microscope, model SU9000. (Ma et al., 2015; Ugwuja et al., 2019).

Gravimetric method

Weight loss analysis was carried out by dipping the weighed coupons in 150 mL of the test solution (1 M HCl) in six different beakers containing different concentrations of 4-HPMAPSA at 303 K in a thermostatic water bath (Ekuma et al., 2017). The coupon was removed from the solution at the end of the exposure period (2 h), washed with 5% chromic acid solution containing 1% silver nitrate and 1% ammonium chloride to stop the corrosion reaction, rinsed in water and dried in acetone and reweighed with analytical weighing balance. This process was repeated at 313, 323 and 333 K. At 303 K, the experiment was repeated, and the coupons were retrieved every 1 h for 5 h. The weight loss, degree of surface coverage, corrosion rate and inhibition efficiency were calculated using equations 1, 2, 3 and 4, respectively (Abdallah and AL Jahdaly, 2015).

$$\Delta W = Wo - W1 \quad (1)$$

$$\theta = \frac{CR_{un} - CR_{in}}{CR_{un}} \quad (2)$$

Corrosion rate = $\Delta W/At$ (3)

$$I.E\% = \frac{CR_{un}-CR_{in}}{CR_{un}}\ x\ 100 \quad (4)$$

Where W_o and W_1 are the initial and final weights of mild steel coupons, CR_{in} and CR_{un} represent the inhibited and the uninhibited corrosion rates, ΔW is the weight loss, A is the surface area of the coupon, and t is the immersion period (Abdallah and AL Jahdaly, 2015).

Results and discussion

Characterisation

From the FTIR spectrum of 4-HPMAPSA (Figure 1), the following peaks represent the functional groups: O-H (3365.90 cm^{-1}), C=N (1693.43 cm^{-1}), C=O (1606.27 and 1083.93 cm^{-1}), C=C (1585.08 and 1512.01 cm^{-1}), C-H bend (1443.35, 1382.93 and 1387.08 cm^{-1}), C-N (1249.83 and 1232.06 cm^{-1}) and C-O (1030.71 cm^{-1}). The FTIR helps to identify the functional groups present in the compound and the formation of the C=N-group at 1693.43 cm^{-1} (Omorogie et al., 2014; Nwanji et al., 2020;

From the X-ray diffraction pattern of 4-HPMAPSA (Figure 2), the clear, sharp Bragg's peaks observed imply that 4-HPMAPSA is crystalline in nature (Omorogie et al., 2014; Sharma, 2015).

Effect of inhibitor concentration and temperature

From the plots of weight loss versus temperature (Figure 3) for mild steel corrosion in 1 M

$HCl_{(aq)}$ in the presence of 4-HPMAPSA, it is clear that an increase in

temperature increased the weight losses of the mild steel, which implies that the temperature

increase accelerated the process (Ekuma et al., 2017). However, with the introduction of 4-HPMAPSA, the weight loss of the mild steel reduced, implying that 4-HPMAPSA decelerated the corrosion of the mild steel in $HCl_{(aq)}$ (Shah et al., 2020). Similar interpretations have been reported (Eddy and Ameh, 2021). The corrosion rate of mild steel in HCl and the inhibition effectiveness of 4-HPMAPSA (Figure 4 and Table 1) for the reactions revealed that an increase in 4-HPMAPSA concentration lowered the corrosion rate and increased the 4-HPMAPSA inhibition effectiveness (Burakov et al., 2018).

Effect of Immersion Time

The plots of the corrosion rate of mild steel against time (Figure 5) in the presence of 4-HPMAPSA at 303 K showed that the corrosion rate increased with an increase in the contact period and decreased with an increase in the 4-HPMAPSA concentration (Ikeuba and Okafor, 2019; Shah et al., 2020).

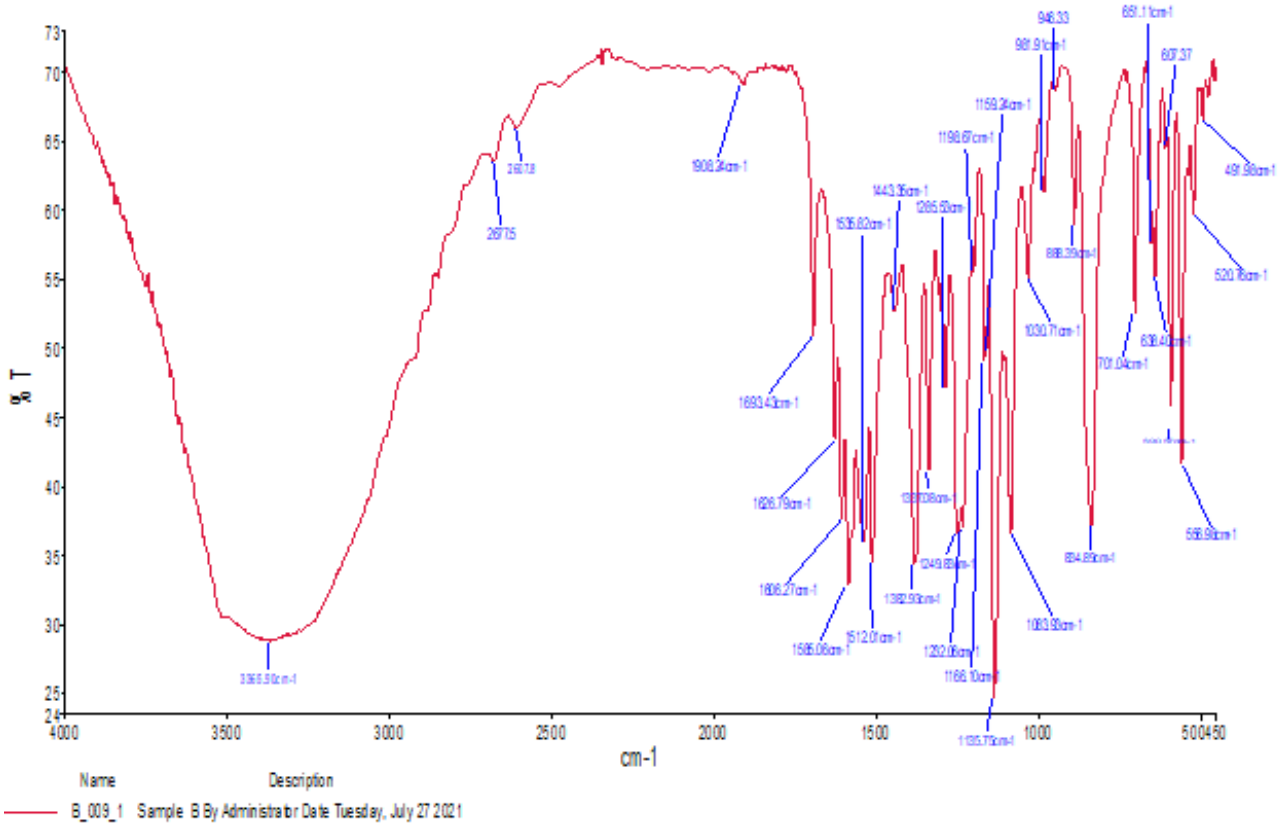

Figure.1: FTIR spectrum of 4-HPMAPSA

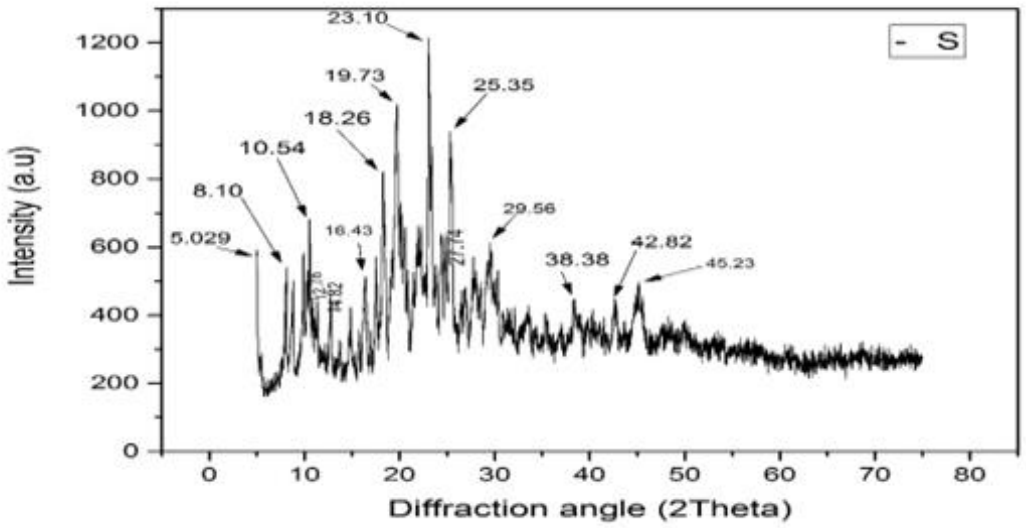

Figure.2: XRD pattern of 4-HPMAPSA

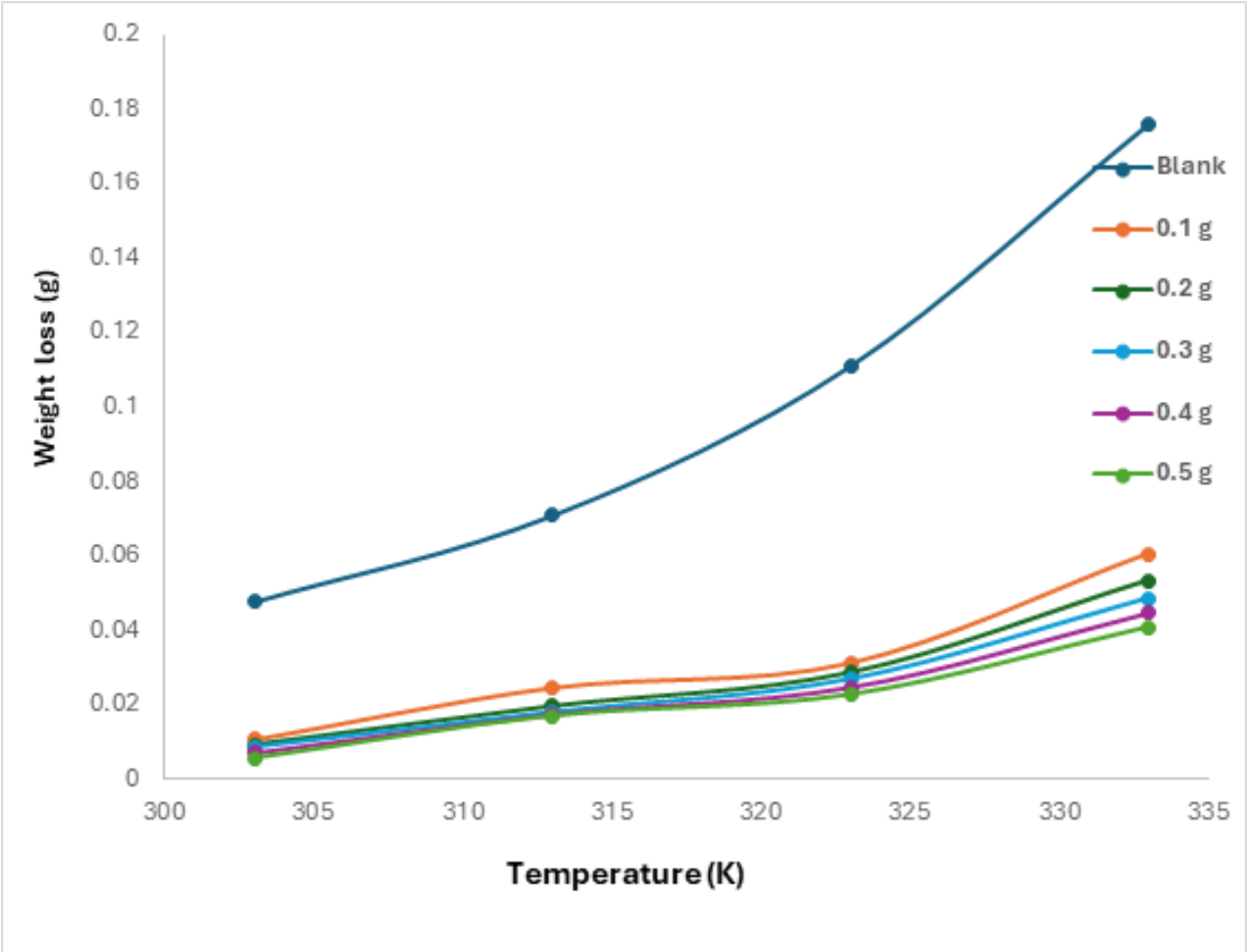

Figure.3: Plots of weight loss against temperature in the presence of 4-HPMAPSA

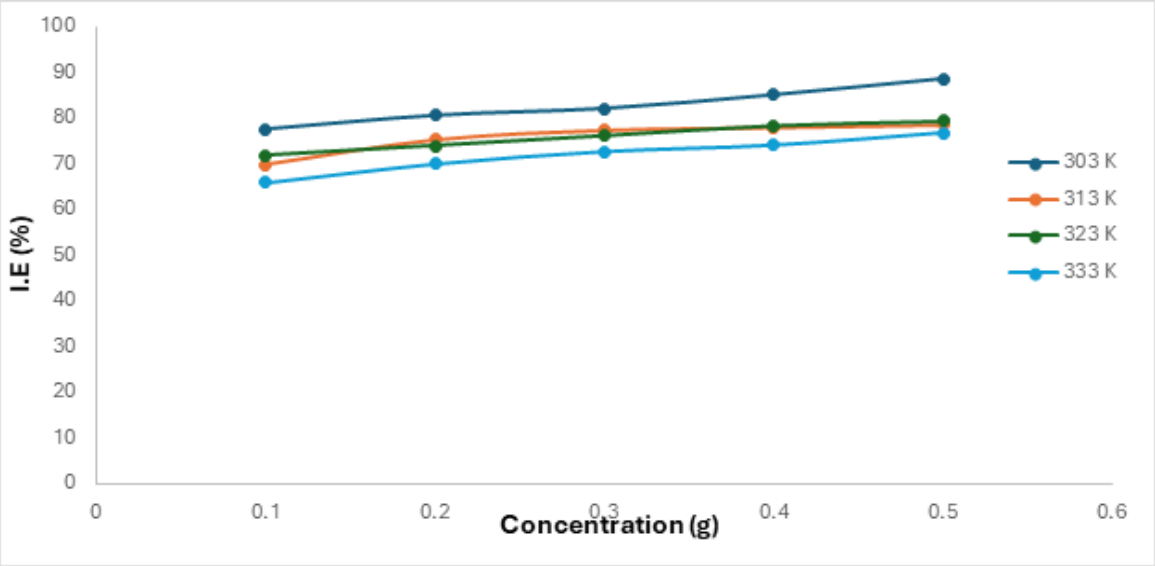

Figure.4: Plots of inhibition efficiency versus 4-HPMAPSA concentrations in 1 M of HCl

Table 1: Corrosion rate, CR ($gcm^{-2}h^{-1}$) and inhibition efficiency (%) of 4-HPMAPSA in 1 M HCl

Conc.(g)	303 K		313 K		323 K		333 K	
	C.R	%I	C.R	%I	C.R	%I	C.R	%I
0.0	0.0020	-	0.0033	-	0.0046	-	0.0073	-
0.1	0.00045	77.5	0.0010	69.7	0.0013	71.7	0.0025	65.8
0.2	0.00039	80.5	0.00082	75.2	0.0012	73.9	0.0022	69.9
0.3	0.00036	82.0	0.00075	77.3	0.0011	76.1	0.0020	72.6
0.4	0.00030	85.0	0.00073	77.9	0.0010	78.3	0.0019	74.0
0.5	0.00023	88.8	0.00071	78.5	0.00095	79.3	0.0019	76.7

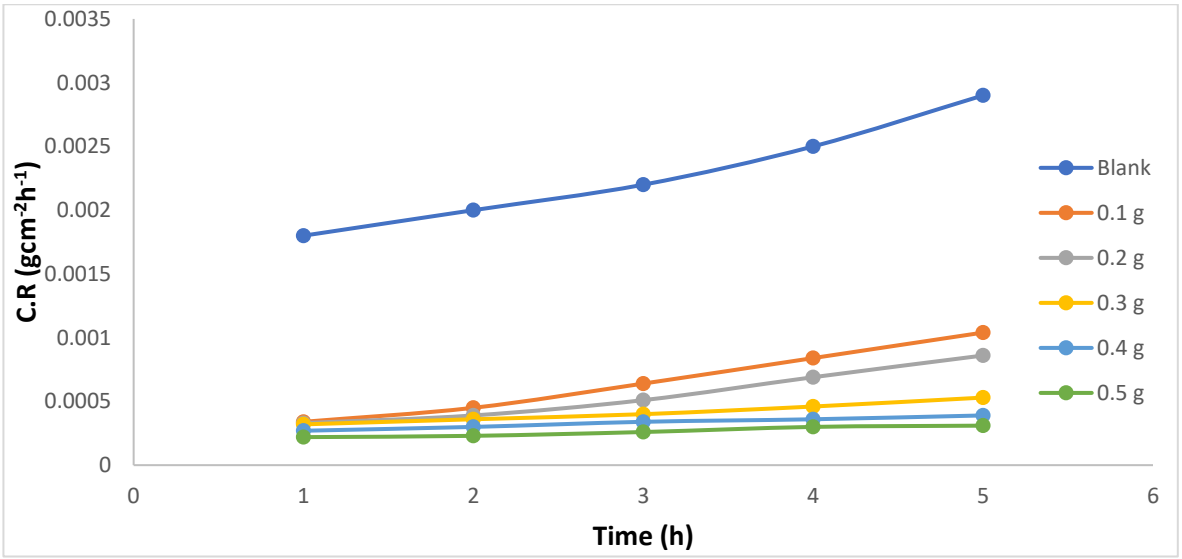

Figure.5: Plots of corrosion rate with time in 1 M HCl with 4-HPMAPSA

Table 2: Corrosion rate, CR ($gcm^{-2}h^{-1}$) and inhibition efficiency (%) of 4-HPMAPSA with time at 303 K

Time (h)	0.0 g C.R	0.1 g		0.2 g		0.3 g		0.4 g		0.5 g	
		C.R	%I	C.R	%I	C.R	%I	C.R	%I	C.R	%I
1	0.0018	0.00034	81.1	0.00033	81.7	0.00032	82.2	0.00027	85.0	0.00022	87.8
2	0.0020	0.00045	77.5	0.00039	80.5	0.00036	82.0	0.00030	85.0	0.00023	88.5
3	0.0022	0.00064	70.9	0.00051	76.8	0.00040	81.8	0.00034	84.5	0.00026	88.2
4	0.0025	0.00084	66.4	0.00069	72.4	0.00046	81.6	0.00036	85.6	0.0003	88.0
5	0.0029	0.00104	64.1	0.00086	70.3	0.00053	81.7	0.00039	86.6	0.00031	89.3

Surface study by scanning electron microscope

Scanning electron micrographs of mild steel in the absence and presence of 4-HPMAPSA in 1 M HCl are shown in Figure 6 (x) and 6(y), respectively and clearly, the corrosion products in the form of pits and flakes can be seen in Figure. 6(x), which implies that the surface was seriously affected by corrosion (Guruprasad et al., 2020). However, with the introduction of 4-HPMAPSA as an inhibitor, Figure. 6(y), it is obvious that the corroding effect is seriously reduced and perhaps, as a result of the 4-HPMAPSA layer formed on the surface (Guruprasad et al., 2020).

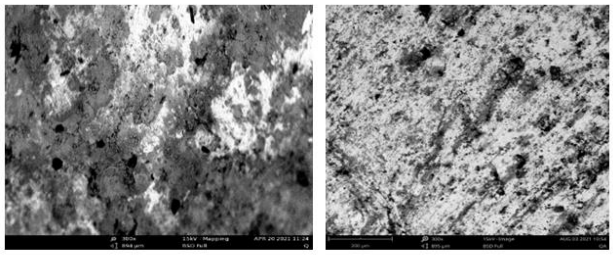

x y

Figure. 6: SEM for the uninhibited and 4-HPMAPSA-inhibited mild steel

Adsorption consideration

The study of 4-HPMAPSA adsorption on mild steel surface using different adsorption isotherm models showed that Langmuir isotherm gave the best fit, and it can be expressed according to equation (5), which simplifies to Equation (6) (Ekuma et al., 2017; Salman et al., 2019).

$$\frac{C}{\theta} = {}^{1}/_{K_{ads}} + C \qquad (5)$$

$$\text{Log}\left(\frac{C}{\theta}\right) = \log C - \log K_{ads} \qquad (6)$$

From equation (6), log(C/θ) against log C should produce a linear graph if the Langmuir isotherm is obeyed [5, 18, 32, 33]. K_{ads} can be determined from the intercept. Figure 7 shows the Langmuir plot for the inhibited reaction of the metal in 1 M $HCl_{(aq)}$ solution. The Langmuir parameters are given in Table 3. The high R^2 values, which ranged from 0.9646 to 0.9999, show that Langmuir isotherm best fitted into the experimental data and also indicate monolayer adsorption of 4-HPMAPSA on the surface (Eddy and Ameh, 2021; Oyedeko et al., 2022).

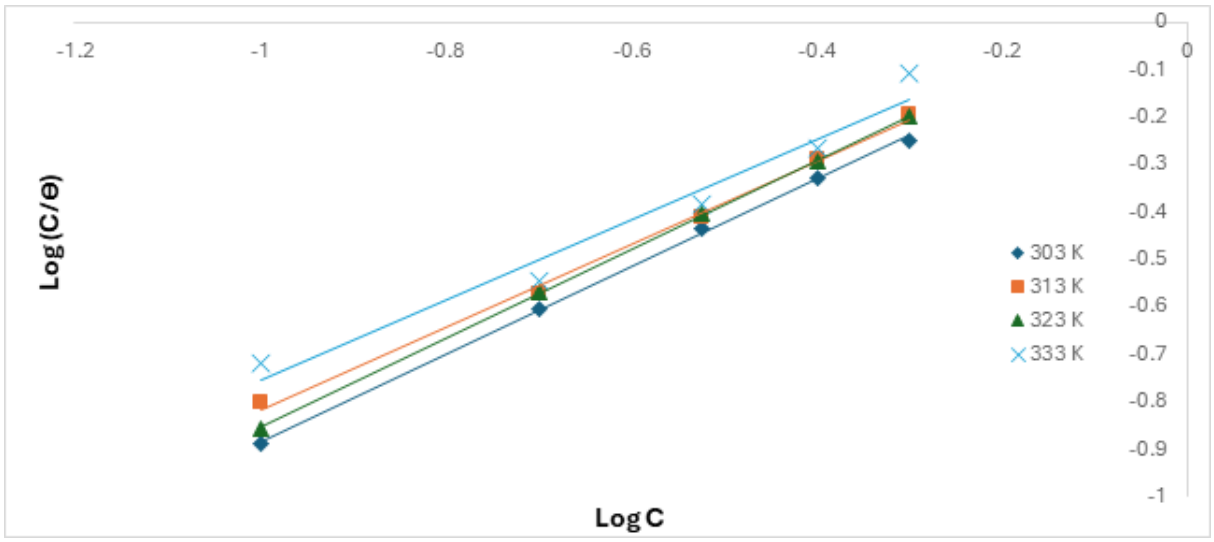

Figure.7: Langmuir plots for 4-HPMAPSA adsorption at different temperatures

Kinetic and thermodynamic considerations

In calculating the activation energy, the Arrhenius equation was used, according to equation (7) and on linearising (7), equation (8) is obtained (Wanees et al., 2017).

$$CR = A\,exp\,(-Ea/RT) \qquad (7)$$

$$Log\ CR = logA - {}^{Ea}/_{2.303\ RT} \qquad (8)$$

From equation (8), log CR versus 1/T produces a linear graph whose slope equals -Ea/2.303R. The determined values of Ea from the slope (Figure 8) were very large and ranged from 35.1 kJ/mol to 52.3 kJ/mol, as shown in Table 4. The Ea value of 35.1 kJ/mol calculated for the uninhibited reaction was significantly smaller than the 47.7 kJ/mol (average) value for the 4-HPMAPSA-inhibited reaction, and this shows that the 4-HPMAPSA mitigated the mild steel corrosion (Wanees et al., 2017; 2019).

The transition state relation (equation 9) was employed for the thermodynamic parameters determination and the free energy, ΔG from equation (10) (Ekuma et al., 2017).

$$Log\left(\frac{CR}{T}\right) = log\frac{R}{Nh} + \frac{\Delta S}{2.303R} - {}^{\Delta H}/_{2.303RT} \qquad (9)$$

$$\Delta G = \Delta H - T\Delta S \qquad (10)$$

Where ΔH is the enthalpy of adsorption, ΔS is the entropy of adsorption, ΔG is Gibbs free energy, R is the gas constant, T is the temperature, N is the Avogadro's number, while h is the Planck's constant.

From equation (9), log (CR/T) versus 1/T produces a linear plot, and its slope is equal to - ΔH/2.303R and the intercept, log R/Nh + ΔS/2.303R (Aslam et al., 2017). Figure 9 shows the Transition state plots, and Table 4 shows the thermodynamic values for 4-HPMAPSA uptake onto the mild steel surface.

The calculated values (Table 4) of ΔH are 42.3 kJ/mol, 43.7 kJ/mol, 43.3 kJ/mol, 46.0 kJ/mol and 49.7 kJ/mol, and this reveals the endothermic nature of the 4-HPMAPSA-inhibited reaction (Lai et al., 2017). The increasing values at higher inhibitor concentrations suggest improved uptake and protective layer formation (Zhou et al., 2016; Gupta et al., 2016). The calculated values of ΔS ranged from 0.252 kJ/mol to 0.272 kJ/mol with an average of 0.259 kJ mol^{-1}. The values of ΔG calculated from equation (10) ranged from -34.1 to -32.7 kJ mol^{-1} at 303 K, -36.6 to -35.4 kJ mol^{-1} at 313 K, -39.1 to -38.2 kJ mol^{-1} at 323 K and -41.6 to -40.9 kJ mol^{-1} for the 4-HPMAPSA-inhibited reaction. The negative values of ΔG implies that the inhibitor adsorption onto the metal surface is spontaneous (Zhou et al., 2015; Gupta et al., 2016), and the range of ΔG values as the temperature increases suggest that the uptake of 4-HPMAPSA on the mild steel surface involved both physical and chemical adsorption (Jagadeesan et al., 2016).

Table 3: Langmuir parameters for 4-HPMAPSA adsorption onto the surface

Temperature (K)	R^2	K_{ads}	Slope
303	0.9994	1.0917	0.9233
313	0.997	1.1327	0.8697
323	0.9999	1.2095	0.9355
333	0.9646	1.2303	0.8453

Table 4: Thermodynamic values for 4-HPMAPSA uptake at different temperatures (in kJ/mol)

Conc. (g)	E_a	ΔH	ΔS	ΔG 303 K	ΔG 313 K	ΔG 323 K	ΔG 333 K
0.0	35.1	32.4	0.231	-37.6	-39.9	-42.2	-44.5
01	45.0	42.3	0.252	-34.1	-36.6	-39.1	-41.6
0.2	46.3	43.7	0.256	-33.9	-36.4	-39.0	-41.5
0.3	46.0	43.3	0.254	-33.7	-36.2	-38.7	-41.3
0.4	48.7	46.0	0.262	-33.4	-36.0	-38.6	-41.2
0.5	52.3	49.7	0.272	-32.7	-35.4	-38.2	-40.9

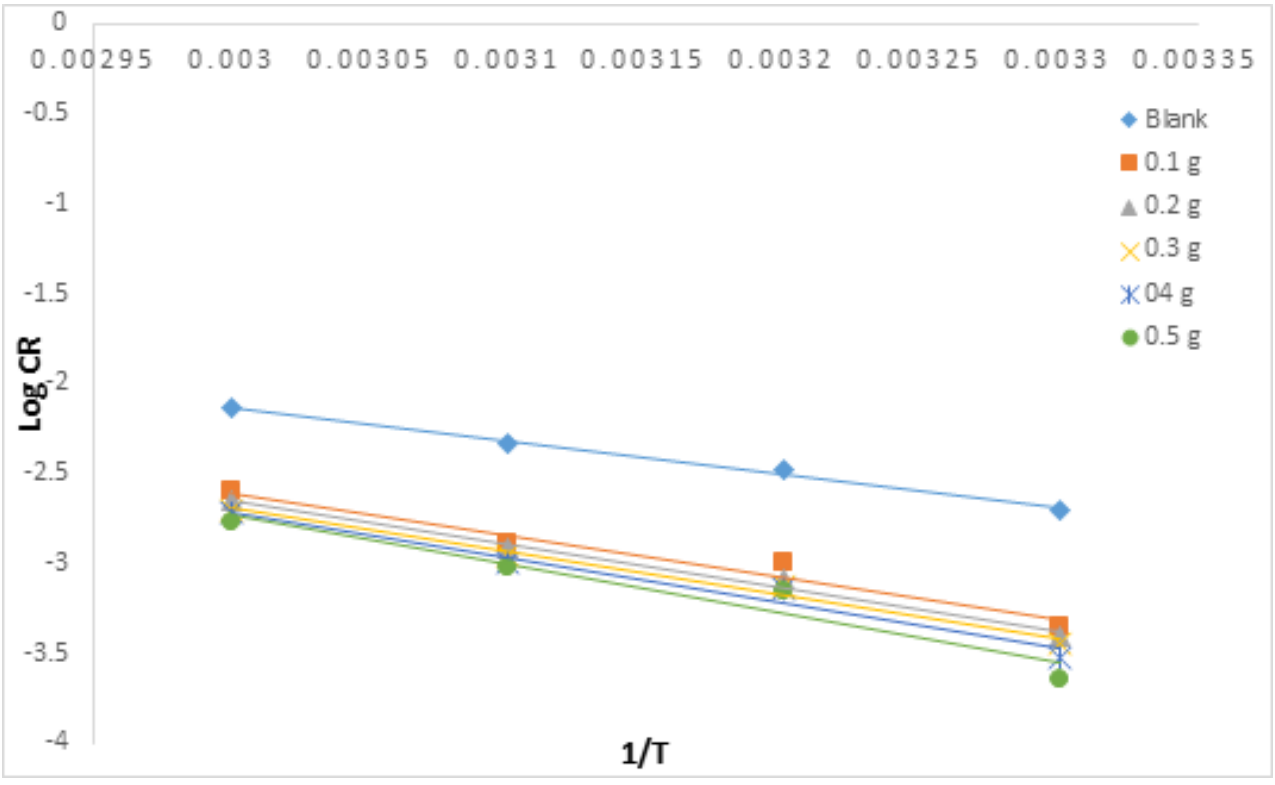

Figure.8: Arrhenius plot for the corrosion inhibition of mild steel with 4-HPMAPSA

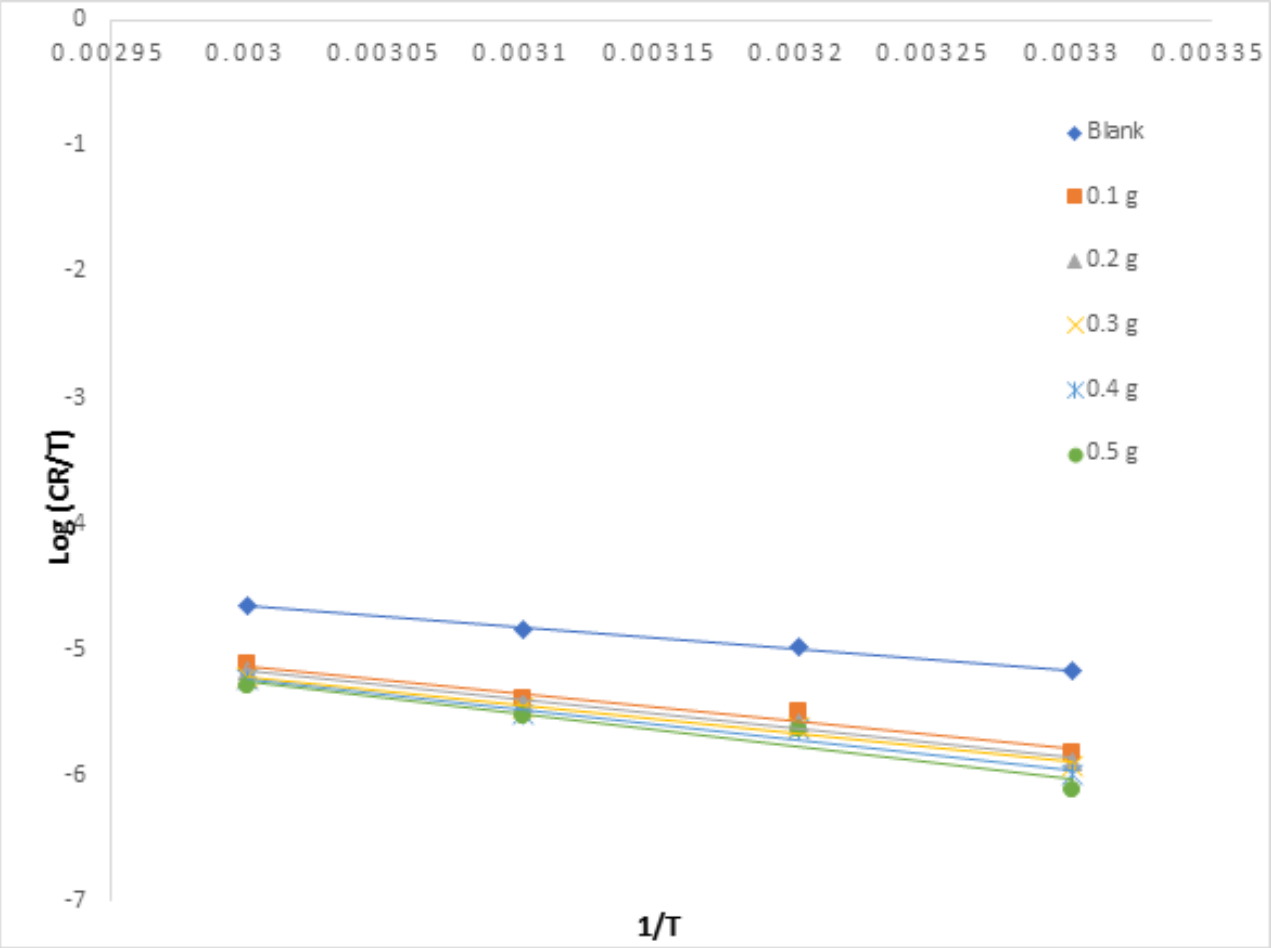

Figure.9: Transition state plot for the inhibition of mild steel corrosion with 4-HPMAPSA

CONCLUSION

N-[(4{[(Z)-(4-hydroxy phenyl) methylidene] amino} phenyl) sulfonyl]acetamide is an effective inhibitor for mild steel in 1 M HCl solution. The inhibition efficiency of 4-HPMAPSA relies on temperature, 4-HPMAPSA concentration and immersion period. The maximum inhibition efficiency was 88.5 % in 0.5 g of 4-HPMAPSA at 303 K. From the thermodynamic consideration, 4-HPMAPSA adsorption on a mild steel surface is endothermic and spontaneous. The result of the adsorption of 4-HPMAPSA on a mild steel surface showed that it obeyed Langmuir isotherm, indicating monolayer layer coverage. This study's results show that 4-HPMAPSA can be gainfully applied by researchers in the corrosion field against corrosion attacks on metallic materials.

RECOMMENDATION

It is recommended that more research be carried out using 4-HPMAPSA as a corrosion inhibitor for mild steel and other metals in different acidic media.

FUNDING

This research received no external funding.

ACKNOWLEDGEMENTS

The authors of this research paper are grateful to their colleagues in the Department of Chemistry, Michael Okpara University, Umudike, Abia State, Nigeria and as well as to the colleagues in the Department of Chemistry, Alex Ekwueme Federal University Ndufu-Alike, Ebonyi State, Nigeria for their support and encouragement respectively.

AUTHORS' CONTRIBUTIONS

Dr. Chikezie Ogueji and Dr. Okoche K. Amadi developed the research plan supervised, and analysed the data. Mr. Divine Chinekwu Oranuka, Chineye Ada Onwuka and Dr. Chikezie Ogueji did the practical work and wrote the manuscript.

DECLARATION OF COMPETING INTEREST

None.

REFERENCES

Abdallah, M. & AL Jahdaly, B.A., (2015). Gentamicin, Kanamycin and Amikacin Drugs as Non-Toxic Inhibitors for Corrosion of Aluminum in 1.0M Hydrochloric Acid, Int. J. Electrochem. Sci., 10, 9808 – 9823. **[Crossref]**

Abdallaha, M., Zaafaranya, I.A. & AL Jahdalya, B.A. (2016). Corrosion Inhibition of Zinc in

Hydrochloric Acid using some Antibiotic Drugs, *J. Mater. Environ. Sci.* 7 (4), 1107-1118.

Ameh, P.O., (2018). Electrochemical and computational study of gum exudates from Canarium schweinfurthii as green corrosion inhibitor for mild steel in HCl solution, 783-795 **[Crossref]**

Aslam, R., Mobin, M., Zehra, S., Obot, I.B. & Ebenso, E.E. (2017). Dialkylcystine Gemini and Monomeric -Alkyl Cysteine Surfactants as Corrosion Inhibitors on Mild Steel Corrosion in 1 M HCl Solution: A Comparative Study, *ACS Omega*, 2(9). **[Crossref]**

Asmara, Y. P. & Kurniawan, T. (2018). Corrosion prediction for corrosion rate of carbon steel in oil and gas environment: A review. Indones. *J. Sci. Technol.* 3, 64–74. **[Crossref]**

Betti, N.,.Al-Amiery, A., KhalidAl-Azzawi, W. & Isahak, W,N. (2023). Corrosion inhibition properties of schif base derivative against mild steel in HCl environment complemented with DFT investigations. *Nature Scientifc Reports* (2023) 13:8979. **[Crossref]**

Burakov, A.E., Galunin, E.V., Burakova, I.V., Kucherova, A.E., Agarwal, S., Tkachev, A.G. & Gupta, V.K. (2018). Ecotoxicology and environmental safety adsorption of heavy metals on conventional and nanostructured materials for wastewater treatment purposes: a review, *Ecotoxicol. Environ. Saf.* 148, 702–712 **[Crossref]**.

Chahul, H.F., Ndukwe, G.I. & Ogwu, D.O. (2018). A thermometric study on the kinetics of the acid dissolution of aluminium in the presence of Napoleonaea imperialis seeds extract and iodide ions, *Ovidius University Annals of Chemistry*, 29(2): 103-109. **[Crossref]**

Eddy, N.O. & Ameh, P.O. (2021). Computational and experimental study on Tapinanthus bangwensis leaves as corrosion inhibitor for mild steel and Al in 0.1 M HCl. *Current Topics in Electrochemistry* Vol. 23, 2021.

Ekuma, F.K., Ogueji, C. & Okoyeagu, A. (2017). Zinc corrosion inhibition by 4-hydroxyl phenyl methylidene-2-(1-phenyl ethylidene) hydrazine carbothioamide (4-HPMHC) and 4-hydroxy phenyl [methylidene] amino-3, 4- dimethyl-5-phenyl cyclo pent-2-en-1-one (4-HPMCP), *J. Chem. Soc. Nigeria*, 42(2), 5-10.

Gupta, V.K., Carrott, P.J.M., Singh, R., Chaudhary, M. & Kushwaha, S. (2016). Bioresource Technology Cellulose: a review as natural, modified and activated carbon adsorbent, *Bioresour. Technol.* 216, 1066–1076. **[Crossref]**.

Guruprasada, A.M., Sachinb, H.P., Swethab, G.A. & Prasannad, B.M. (2020). Corrosion inhibition of zinc in 0.1 M hydrochloric acid medium with clotrimazole: Experimental, theoretical and quantum studies. Surfaces and Interfaces, 19 (2020) 100478. **[Crossref]**.

Hegazy, M.A., Abdallah, M., Awad, M.K. & Rezk, M. (2014). Part I: Experimental Results, *Corros. Sci.*, 81, 54. **[Crossref]**

Ikeuba, A.I. & Okafor, P.C. (2019). Green corrosion protection for mild steel in acidic media: saponins and crude extracts of Gongronema latifolium. Pigment & Resin Technology, 48(1):57-64. **[Crossref]**

Ikeuba, A.I., Ita, B.I., Etiuma, R.A., Bassey, V.M., Ugi, B.U. & Kporokpo, E.B. (2015). Green Corrosion Inhibitors for Mild Steel in H_2SO_4 Solution: Flavonoids of Gongronema latifolium, *Chemical and Process Engineering Research*, 34, www.iiste.org ISSN 2224-7467 (Paper), ISSN 2225-0913 (Online).

Jagadeesan, S., Sowmiya, M., Sounthari, P., Parameswari, K., Chitra, S., Senthilkumar, K., 2016. N-heterocycles as corrosion inhibitors for mild steel in acid medium, Journal of Molecular Liquids, 216:42-52. **[Crossref]**

Kadhum, A.H., Mohamad,A.B., Hammed, LA., Al-Amiery, A.A., San, N.H. & Musa, A.Y. (2014). Inhibition of Mild Steel Corrosion in Hydrochloric Acid Solution by New Coumarin, *Material*, 7, 4335-4348, **[Crossref]**

Kavitha, V. & Gunavathy, N. (2014). Evaluation of Daucus carota aerial extract as corrosion inhibitor for mild steel in hydrochloric acid medium, *International Journal of Research in Advent Technology,* 2(7) 146- 154.

Kumari, P., Rao, S.A., & Shetty, P. (2014). Corrosion inhibition of mild steel in 2 M HCl by Schiff base derivative. Procedia material science, 5:499-507. **[Crossref]**

Lai, C., Xie, B., Zou, L., Zheng, X. & Ma, X. (2017). Adsorption and Corrosion Inhibition of Mild Steel in Hydrochloric Acid Solution by S-allyl-O,O'-dialkyldithiophosphates, 7, **[Crossref]**

Ma, J., Zhou, L., Dan, W., Zhang, H., Shao, Y., Bao, C. & Jing, L. (2015). Novel magnetic porous carbon spheres derived from chelating resin as a heterogeneous Fenton catalyst for the removal of methylene blue from aqueous solution, *J. Colloid Interface Sci,* 446, 298–306 **[Crossref]**.

Nwanji, O.L., Omorogie, M.O., Olowoyo, J. O. & Babalola, J.O. (2020). "Remediation of industrial

dye by Fentonactivated biogenic waste, *Surfaces and Interfaces*, 20, 100555. **[Crossref]**.

Ofuyekpone, O.D., Utub, O.G. & Onyekp, B.O. (2021). Corrosion inhibition for alloy 304L (UNS S30403) in H2SO4 1M solution by Centrosema pubescens leaves extract. Applied Surface Science Advances, 3(2021) 100061. **[Crossref]**

Omorogie, M.O., Babalola, J.O., Unuabonah, E.I. & Gong, J.R. (2014). Solid phase extraction of hazardous metals from aqua system by nanoparticle-modified agrowaste composite adsorbents. J Environ Chem Eng, 2(1), 675–684.

Omorogie, M.O., Babalola, J.O., Unuabonah,E.I. & Gong, J.R. (2014). Hybrid materials from agro-waste and nanoparticles: implications on the kinetics of the adsorption of inorganic pollutants. Environ Technol, 35(5), 611–619.

Onwu, F.K., Ogueji, C. & Mgbemena, N.M. (2016). Inhibition of Corrosion of Zinc in H_2SO_4 Medium by the Schiff Base, 4-Hydroxy Phenyl Methylidene-2-(l-Phenyl Ethylidene) Hydrazine Carbothioamide (4-HPMHC), *DerChemica Sinica*, 7(4), 13-20.

Oyedeko, K., Lasisi, M., & Akinyanju, A. (2022). Study of Blend of Extracts from Bitter Leaf (Vernonia Amygdalina) Leaves and Banana (Musa Acuminata) Stem as Corrosion Inhibitor of Mild steel in Acidic Medium. Eur J Eng Technol Res., 7(1), pp. 1–9. **[Crossref]**

Pathak, R. K. & Pratiksha, M. (2016). Drugs as corrosion inhibitors: a review, *Int. J. Sci. Res.* 5 (4) (2016) 671–677. **[Crossref]**

Paul, P.K., Mehta, R.K., Yadav, M. & Obot, I.B. (2021). Theoretical, electrochemical and computational inspection for anti-corrosion activity of triazepine derivatives on mild steel in HCl medium. *Journal of Molecular Liquids*. **[Crossref]**

Salman, T. et al., 2019. Novel ecofriendly corrosion inhibition of mild steel in strong acid environment: Adsorption studies and thermal effects. Int J Corros Scale Inhib., 8(4), pp. 1123–1137. **[Crossref]**

Shah, N.S., Ali, J., Sayed, M., Ul, Z., Khan, H., Iqbal, J. & Arshad, S. (2020). Synergistic effects of H_2O_2 and $S_2O_8^{2-}$ in the gamma radiation induced degradation of congo-red dye: kinetics and toxicities evaluation, *Sep. Purif. Technol.* 233 (2020) 115966 **[Crossref]**.

Sharma, A., (2015). Azadirachta indica (Neem) leaf powder as a biosorbent for removal of Cd(II) from aqueous medium, Journal of Hazardous Materials, 125(1-3), 102- 112. **[Crossref]**

Ugwuja, C.G., Adelowo, O., Ogunlaja, A., Omorogie, M.O., Olukanni, O., Ikhimiukor, O., Iermak, I., Kolawole, G., Guenter, C. & Taubert, A. (2019). Visible-light mediated photodynamic water disinfection@ bimetallic doped hybrid clay nanocomposites, ACS Appl Mater Interfaces 11(28), 25483–25494. **[Crossref]**

Wanees, A. S.; Radwan, A. B.; Alsharif, M. A. & Abd El Haleem, S. M. (2017). Initiation and Inhibition of Pitting Corrosion on Reinforcing Steel under Natural Corrosion Conditions. Mater. Chem. Phys. 2017, 190, 79–95. **[Crossref]**.

Wanees, S.A., & Seda, S. H. (2019). Corrosion inhibition of zinc in aqueous acidic media using a novel synthesised Schiff base – an experimental and theoretical study. *Journal of Dispersion Science and Technology*, **[Crossref]**

Zhou, L., Ma, J., Zhang, H., Shao, Y. & Li, Y. (2015). Fabrication of magnetic carbon composites from peanut shells and its application as a heterogeneous Fenton catalyst in removal of methylene blue, *Appl. Surf. Sci.* 324, 490–498. **[Crossref]**